PREDICTION OF INTRINSIC PERMEABILITIES WITH LATTICE BOLTZMANN METHOD

Luís Orlando Emerich dos Santos
Federal University of Santa Catarina - Florianópolis - Santa Catarina - Brazil
emerich@lmpt.ufsc.br

Carlos Enrique Pico Ortiz
Federal University of Santa Catarina - Florianópolis - Santa Catarina - Brazil
capico@lmpt.ufsc.br

Henrique Cesar de Gaspari
Federal University of Santa Catarina - Florianópolis - Santa Catarina - Brazil
henrique@lmpt.ufsc.br

Guilherme Eller Haverroth
Federal University of Santa Catarina - Florianópolis - Santa Catarina - Brazil
haverroth@lmpt.ufsc.br

Paulo Cesar Philippi
Federal University of Santa Catarina - Florianópolis - Santa Catarina - Brazil
philippi@lmpt.ufsc.br

Abstract. *In this work, we use the Lattice Boltzmann method to simulate flows through porous media. After a brief description of the method, we present flow simulations through simple three-dimensional geometries. These simulations are compared with analytical solutions aiming to validate the method. More realistic geometries are obtained by means of reconstruction methods from bi-dimensional images of brazilian sandstones. Intrinsic permeabilities predicted from simulations in reconstructed geometries are compared with experimental data.*

Keywords: *Porous media, Intrinsic permeability, Lattice Boltzmann method*

1. Introduction

Prediction of equilibrium and transport properties of porous media is a long-standing problem of great practical interest, specially in petroleum reservoir engineering. The permeability is an important physical property of a porous medium and its accurate determination is vital to the design and application of oil production schemes. Although, the complex geometry of porous structure greatly difficult to simulate physical processes at pore level. The Lattice Boltzmann method (LBM) provides an alternative to traditional methods of computational fluid dynamics, which are based on the discretization of Navier-Stokes equation. LBM, on the other hand is based on the Boltzmann transport equation and is less sensible to the complexity of the porous media geometry. It has been subjected to many developments in the last years, and applied with considerable success to several problems in computational physics (see, for instance, Succi, 2001).

2. The Lattice Boltzmann Method

2.1 Microscopic dynamics

Three-dimensional physical space is considered to be a cubic lattice where each site $\mathbf{X}$ has b_m neighbors (see Fig. 1). Each site is characterized by a particle distribution function $N_i(\mathbf{X}, T)$ which evolves according to the Lattice Boltzmann Equation:

$$N_i(\mathbf{X} + \mathbf{c}_i, T + 1) = N_i(\mathbf{X}, T) + \Omega_i, \tag{1}$$

where T is the time variable, the index i indicates the neighbor, $\mathbf{c}i$ is a velocity vector pointing to neighbor i ($i = O$ refers to the rest particle distribution). The term in the right side is called collision term and is written in such way that

$$\sum_i \Omega_i = 0, \tag{2}$$

$$\sum_i \Omega_i \mathbf{c}_i = 0, \tag{3}$$

in order to preserve the mass and momentum of each site.

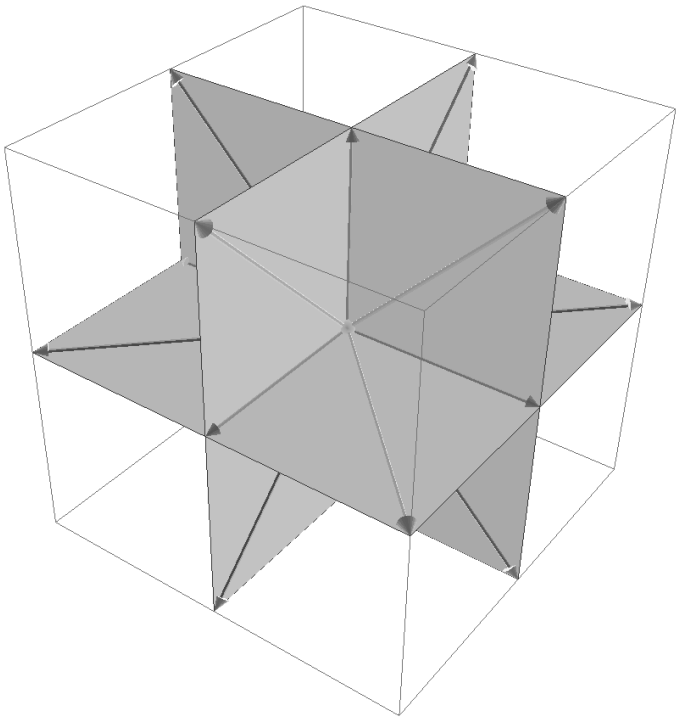

Figure 1. Tridimensional lattice with 19 velocities.

The evolution of the model, given by Eq. (1), can be split in two processes. In the first, designated as collision, the distribution function $N_i(\mathbf{X}, T)$ is changed by the action of the collision operator. In the second process, called propagation, the values N_i are propagated to the neighboring sites, in accordance with the direction of the vector c_i. The mass and momentum variables are defined with the help of the distribution function:

$$\sum_{i=0}^{b} N_i = \rho, \tag{4}$$

$$\sum_{i=0}^{b} N_i \mathbf{c}_i = \rho \mathbf{u}. \tag{5}$$

2.2 The BGK Collision Term

In present paper a single-relaxation-time approximation for the collision operator is used (see Qian et al., 1992):

$$\Omega_i = \frac{N_i^{eq} - N_i}{\tau} \tag{6}$$

where τ is the relaxation time and N_i^{eq}, the equilibrium distribution, is determined in order to obtain the desired macroscopic equations. The rate of change toward the equilibrium distribution is imposed to produce the viscosity of the fluid, which is the only macroscopic property related to collisions in single-fluid flows.

2.3 Equilibrium distributions

When equilibrium is reached collision process should not affect the particle distribution. Therefore, the equilibrium distributions N_i^{eq} must be specified by the collisional invariants ρ and $\rho\mathbf{u}$. To the case of small $\mathbf{u}$, it can be written:

$$N_i^{eq}(\rho, \mathbf{u}) = A_i + B_{i\alpha}\mathbf{u}_\alpha + D_{i\alpha\beta}\mathbf{u}_\alpha\mathbf{u}_\beta, i = 1, ..., bm, \tag{7}$$

where b_m indicates the number of directions of the lattice and repeated indexes indicate summations. The parameters Ai and $B_{i\alpha}$ can be determined by imposing mass and momentum conservation. The remained parameter, $D_{i\alpha\beta}$, is chosen in order to obtain the desired macroscopic hydrodynamic equations. The final form of the equilibrium distribution are:

$$N_0^{eq} = \frac{\rho}{3} - \frac{\rho}{2}u^2, \tag{8}$$

for the rest particles,

$$N_i^{eq} = \frac{\rho}{18} + \frac{\rho}{6}\mathbf{c}_i \cdot \mathbf{u} + \frac{\rho}{4}(\mathbf{c}_i \cdot \mathbf{u})^2 - \frac{\rho}{12}u^2, \tag{9}$$

for moving particles along the main axes, and

$$N_i^{eq} = \frac{\rho}{36} + \frac{\rho}{12}\mathbf{c}_i \cdot \mathbf{u} + \frac{\rho}{8}(\mathbf{c}_i \cdot \mathbf{u})^2 - \frac{\rho}{24}u^2, \tag{10}$$

for particles moving along the diagonals ($|\mathbf{c}_i| = \sqrt{2}$).

2.4 Scaling to physical variables

Using h and δ as, respectively, a spatial and a time scale,

$$\mathbf{x} = h\mathbf{X}, \tag{11}$$

$$t = \delta T, \tag{12}$$

when h and δ are small, $\mathbf{x}$ and t may be considered as physical variables, varying continuously in the spatial and time domain of the physical system to be described.

2.5 Hydrodynamic LB equations

Using Chapman-Enskog method in the Lattice-Boltzmann equation, in the limit of low Knudsen number $K_n = \frac{h}{L} = \delta\Gamma/ << 1$, where L is a characteristic length and Γ is a characteristic time, and neglecting terms beyond second order, leads to

$$\partial_t(\rho) + \partial_\beta(\rho u_\beta) = 0, \tag{13}$$

$$\partial_t(\rho u_\alpha) + \partial_\beta(\rho u_\alpha u_\beta) = -\partial_\alpha(p) + \nu\partial_\beta\left[\partial_\beta(\rho u_\alpha) + \partial_\alpha(\rho u_\beta)\right], \tag{14}$$

where the pressure p and the kinematic viscosity ν are given by

$$p = \frac{1}{3}\rho, \tag{15}$$

$$\nu = \frac{1}{3}(\tau - 1/2). \tag{16}$$

The mass balance equation is, exactly, the same equation obtained in classical hydrodynamics. Considering low Mach number (p constant), the obtained momentum balance equation will be, clearly, in agreement with the Navier-Stokes equation.

2.6 Boundary conditions

At the solid surfaces were imposed bounce back boundary conditions for particle distributions, i. e., all particle that would hit the walls in the propagation step reverses its direction in this step. This boundary condition assures the non-slip boundary condition near the walls and, although there are other ways to ensure non-slip condition (Inamuro et al., 1996), it was chosen due to its simplicity .Two boundary conditions were applied at the inlet and the outlet of the domain in the flow direction: (a) periodic boundary condition were applied by imposing that any fluid exiting in one of the edge (say, in the exit) reenters in the other edge (the entrance); (b) null derivative condition in the direction of the flow were obtained by imposing that sites in the entrance (for instance, x = 0) assume the velocity of the adjacent sites (x = 1), and analogous were done in the outlet. In case (a), in order to force the flow, a fixed amount of momentum is added at each site. In case (b) the flow is obtained by imposing a pressure gradient.

3. Simulations

Darcy's law relates the flow rate **J** of a fluid with the force applied to it. In symbols it can be written,

$$\mathbf{J} = \frac{k}{\mu}(\rho\mathbf{g} - \nabla p), \tag{17}$$

where μ is the viscosity of the fluid, $\mathbf{g}$ is the gravitational force density, ∇p is the pressure gradient, and k is the permeability coefficient.

In a steady flow the force applied to the fluid equals the momentum lost in the solids surfaces. In the simulations we prefer to compute the total amount of momentum lost in the propagation step to calculate the permeability, so the same algorithm can be applied, being unimportant if a force (say, $\rho\mathbf{g}$) or a pressure gradient (or both) are impelling the flow.

3.1 Flow through capillaries

In order to validate our procedure to predict intrinsic permeabilities we simulate the flow in capillary tubes. Considering a parabolic velocity profile it can be shown (see Bear, 1988) that

$$k = \frac{D^2}{32} \tag{18}$$

where is the D diameter of the capillary. Using periodic boundary conditions, it was necessary to simulate the flow only in a section of capillary, since the velocity field is the same all along the tube (see Fig. 2).

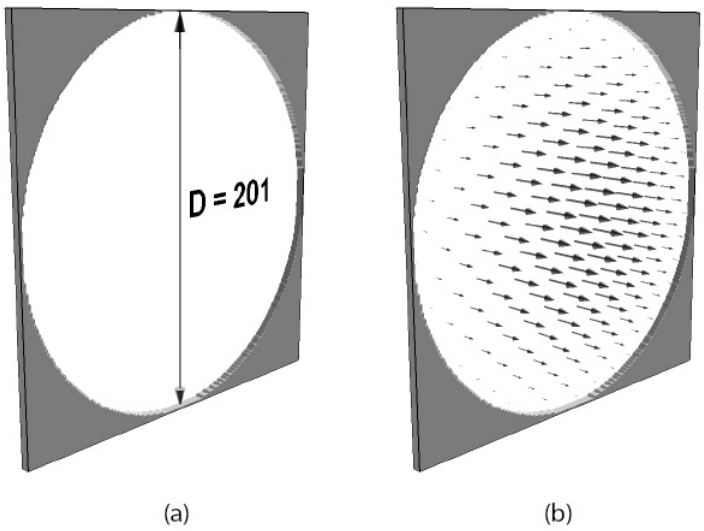

Figure 2. (a) A section of a capillary with $D = 201$ lattice units. (b) Velocity field in the section.

The results of the simulations for several diameters D and comparisons with theoretical predictions are shown in Table 1. It can be seen that, as D increases, diminishing discretization effects, simulated results approaches the theoretical ones.

Table 1. Comparison between theoretical and simulated results for capillaries.

Diameter	k theoretical	k simulated	error (%)
25	19.53	20.26	3.7
49	75.03	76.44	1.88
99	306.28	309.583	1.08
201	1262.53	1269.66	0.56

3.2 Flow through a periodic array of spheres

Considering a Stokes flow, Larson and Higdon (1988) calculate the permeability of periodic array of spheres, in which the radius of the spheres is allowed to increase past the point of touching, forming a consolidated medium. To compare their results with our simulations we employ simple cubic arrays (see Fig. 4(a)) with periodic boundary conditions. Due to the symmetry, using periodic boundary conditions, its necessary to simulate only one cell (Fig. 4(b)). The theoretical and simulated results are showed in table 2. The small differences between them can be attributed to discretization effects, decreasing as the cell length and diameters are made greater.

3.3 Flow through reconstructed porous media

Several simulations were performed to calculate intrinsic permeability of Brazilian sandstones. Simulations start from three-dimensional representations of the porous structure, reconstructed from petrographic thin plates by using the method propose by Liang et al.(1988). The method starts with a set of binary two-dimensional images, three-dimensional reconstruction is based on the generation of three-dimensional stochastic realizations, preserving the statistical moments of phase function, which are measured on the target binary images. Present reconstruction method preserves the two first

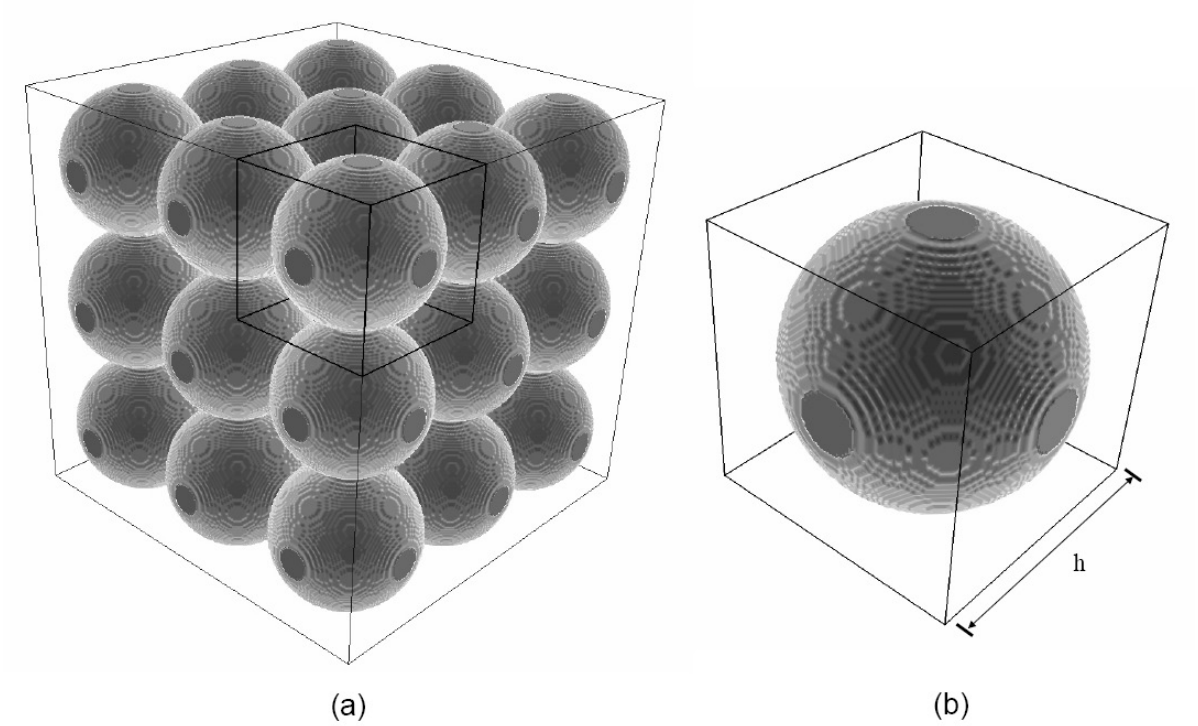

Figure 3. (a) Simple cubic array of spheres. (b) A single sphere in detail.

Table 2. Comparison between theoretical and simulated results for periodic arrays of spheres.

Diameter	Cell lenght (h)	k theoretical	k simulated	error (%)
22	21	0.67098	0.69457	3.5
44	42	2.7763	2.7618	0.52
66	63	6.1671	6.1310	0.58
112	107	17.978	17.924	0.3
138	131	25.114	25.002	0.45

moments of the phase function: porosity and auto-correlation. A typical reconstructed image is shown on Fig. **??**. Table 2 gives some simulation results and comparison with experimental data furnished by CENPES/ Petrobras, which also furnishes the source digital images. All simulations were performed in cubic reconstructed structures with 200^3 voxels, each pixel corresponding to $4.545\mu m$.

The comparison with experimental results (see table 3) shows good predictions of permeability (BOO6, BOOS, BOO9), considering the difficult involved in the reconstruction process and in the simulations of flows in the reconstructed image. The results showing considerable disagreement with experimental data (BOO5 and BOO7) are, possibly, consequence of the small volume of the structures used in the simulations. More studies are demanded to determine the minimum size necessary to adequately represent the porous structure.

Table 3. Comparison between experimental and simulated results.

Sample	Porosity ϕ	k experimental (mDa)	k simulated (mDa)
B005	21.5	152.5	482
B006	22	197.5	233.2
B007	26.7	407.8	1940
B008	25.3	540	435
B009	27.6	642	902

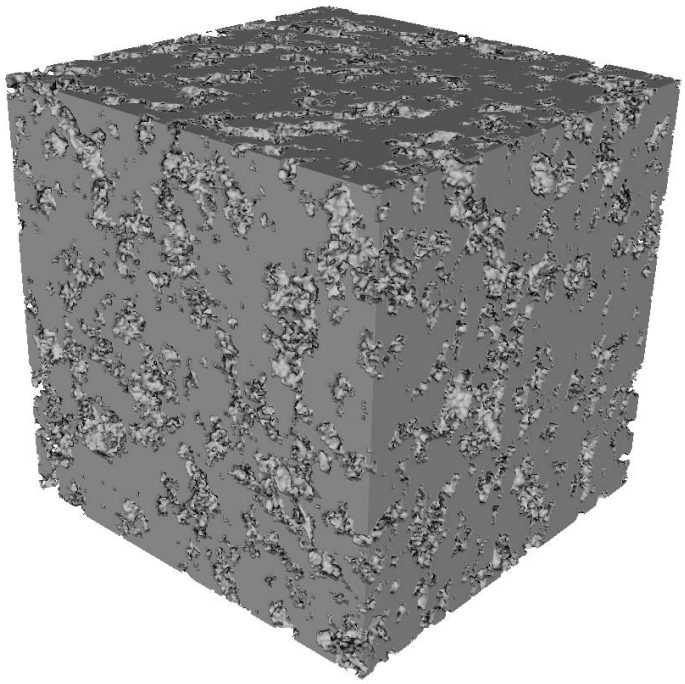

Figure 4. Porous media reconstructed with Truncated Gaussian Method.

4. Conclusion

The lattice Boltzmann method was presented as a tool for performing fluid dynamic simulations in porous media. The macroscopic behavior of the model was discussed, and simulation results were presented. Flow simulations in simple 3D geometries showed excellent results. Simulations in reconstructed 3D geometries showed good and not so good results; which can be attributed to the small size of structures used in the simulations.

5. Acknowledgments.

The authors would like to acknowledge CENPES/ PETROBRAS (Centro de Pesquisas e Desenvolvimento Leopoldo A. Miguez de Mello) for providing the images and the experimental data for reservoir rocks. The authors also acknowledge the financial support of CNPq (Conselho Nacional de Desenvolvimento Científico e Tecnológico), ANP (Agência Nacional do Petróleo) and FINEP (Financiadora de Estudos e Projetos).

6. References

Succi, S., 2001, "The Lattice Boltzmann Equation for Fluid Dynamics and Beyond", Oxford University Press, Oxford.

Qian, Y. H., d'Humieres D., Lallemand P., 1992, "Lattice BGK Models for Navier- Stokes Equation", Europhys. Lett. 17, pp. 479-484.

Inamuro, T., Yoshino, M., Ogino, F., 1995, "Non-slip boundary condition for lattice Boltzmann simulations", Physics of Fluids, vol. 7, No.12, pp. 2928-2930.

Bear, J., 1988, "Dynamics of fluids in porous media", Dover, Mineola, United States of America, p 162.

Larson, R. E. and Higdon J. J. L., "A periodic grain consolidation model of porous media" Phys. Fluids A, vol. 1, No.1, pp. 38-46.

Liang, Z. R., Femandes, C. P., Magnani, F.S. and Philippi, P. C., 1998, "A Reconstruction Technique of3-DPorous Media by using Image Analysis and Using Fourier Transform", Journal ofPetroleum Science and Engineering, vol. 21, No. 3-4, pp. 273-283.

7. Responsibility notice

The author(s) is (are) the only responsible for the printed material included in this paper